Automotive Innovation (2025) 8:549–555
https://doi.org/10.1007/s42154-025-00391-7

Operation of a Passive Fuel Cell Under Sub-Zero Environment Conditions

Xingyi Shi[1,3,4] · Xiaoyu Huo[1] · Yuran Bai[1] · Lizhen Wu[1] · Yun Liu[1] · Wenzhi Li[1] · Yichen Dai[1] · Yu Hao Chang[1] · Oladapo Christopher Esan[1] · Qixing Wu[2] · Liang An[1,4]

Received: 26 November 2024 / Accepted: 17 April 2025 / Published online: 14 July 2025

Abstract

In the last decade, liquid fuel cells with their numerous advantages have gained widespread attention across the globe. However, it is a prerequisite for the fuel cells to attain an all-climate operation ability before realizing broad and extensive applications. To date, conventional liquid fuel cells always require pre-heating strategy or auxiliary heating equipment before they can operate in sub-zero environments, which makes the system bulky and prolongs its response time. The recently proposed and demonstrated novel electrically rechargeable liquid fuel (e-fuel), is considered to be a potential solution for powering fuel cells in various environments, particularly under sub-zero conditions. Using the e-fuel, a passive liquid fuel cell is designed, fabricated, and examined from 23 to – 20 °C. The cold-start free fuel cell is demonstrated to attain a peak power density of 110.34 mW· cm^{-2} at − 20 °C. Furthermore, to demonstrate its capability for commercial application, a two-cell stack has been developed to power a toy train, which not only demonstrates the superior scalability of this system, but also presents it as a feasible device for power generation in extreme environments.

Keywords E-fuel · Vanadium · Fuel cell · Sub-zero environment · Extreme conditions

Abbreviations

DLFC	Direct liquid fuel cell
E-fuel	Electrically rechargeable liquid fuel
MEA	Membrane electrode assembly
PPD	Peak power density

1 Introduction

The continuous and enormous growth in global energy demand over the last decade has made the evolution of sustainable power generation systems, a pressing mission for the future society. As a promising green power generation technology, the fuel cell has demonstrated its great potential for application in various practical scenarios, from mobile devices to stationary power stations [1, 2]. Among diverse kinds of fuel cells, the direct liquid fuel cell (DLFC) is believed to be a promising competitor [3–5]. It directly converts the chemical energy in liquid fuels into electricity through electrochemical reaction, thereby allowing the system with many superiorities [6]. However, the current performance of conventional DLFCs is still unsatisfactory, which has greatly restricted their commercialization progress. The operation of DLFCs involves a series of heat and mass transport processes and electrochemical reactions, all of which require a suitable operating temperature, leading to a bulky and low-efficiency system [7]. On top of that, the sluggish reaction kinetics of common alcoholic fuels is another major issue that results in high catalyst cost and limited operational temperature range, confining the application scenarios of the system [8, 9]. The successful operation of fuel cells in sub-zero environments, without

✉ Qixing Wu
qxwu@szu.edu.cn

✉ Liang An
liang.an@polyu.edu.hk

1 Department of Mechanical Engineering, The Hong Kong Polytechnic University, Hung Hom, Kowloon, Hong Kong SAR 999077, China

2 Shenzhen Key Laboratory of New Lithium-Ion Batteries and Mesoporous Materials, College of Chemistry and Environmental Engineering, Shenzhen University, Shenzhen Province 518060, Guangdong, China

3 City University of Hong Kong (Dongguan), Dongguan 523808, Guangdong Province, China

4 Research Institute for Smart Energy, The Hong Kong Polytechnic University, Hung Hom, Kowloon, Hong Kong SAR 999077, China

the implementation of any pre-heating strategies or auxiliary equipment, remains a significant challenge for both hydrogen–oxygen and traditional liquid fuel cells. It is thus critical to identify and adapt other potential liquid fuels with better reaction kinetics in fuel cells to achieve all-climate operation, especially in sub-zero environments.

Lately, a novel electrically rechargeable liquid fuel (e-fuel) has been demonstrated as an alternative to conventional alcoholic liquid fuels, which has been found to provide outstanding cell performance [10]. Potentially, this e-fuel can be created from a variety of materials while owning a superior electrochemical reaction kinetics, even without any noble metal catalysts. Furthermore, unlike traditional alcoholic fuels, the e-fuel is rechargeable, which allows it to be reused for many cycles, greatly lowering its manufacturing costs and mitigating the environmental impacts. In one previous study, using an e-fuel composed of vanadium ions, a liquid fuel cell has been proven to be able to operate at − 20 °C without any pre-heating strategies [11]. However, the water generated on the cathode side would unavoidably lead to ice formation issue and influence the system long-term stability [12, 13]. It is reported that, in sub-zero environments, ice formation is prone to occur on the cathode side, which can obstruct the delivery of oxidant through the catalyst layer, thereby inhibiting electrochemical reactions by limiting the availability of reactants and diminishing the active surface area. Furthermore, this phenomenon may even lead to internal short circuits, and raise significant safety concerns [14, 15]. Therefore, in this study, in an attempt to eliminate the ice formation issue, another liquid e-fuel with low freezing point is employed as oxidant to replace the oxygen during the cell operation. It is reported to have a low freezing point of ~ − 30 °C granting it to be applicable under sub-zero conditions. Furthermore, to ensure the feasibility of this system as a power source for mobile devices, a passive fuel cell design is adopted freeing the cell from any additional devices, including pumps and heaters. The cell is found to be capable of attaining a peak power density (PPD) of 110.34 $mW{\cdot}cm^{-2}$ even at – 20 °C. In addition, a two-cell stack has also been developed for powering a toy train, which demonstrates the scalability and applicability of this system. The demonstrated e-fuel cell is envisaged to propel this technology to achieve further breakthroughs and broaden its applications, especially in extreme operating conditions, notably for power generation under all-climate conditions.

2 Working Principle

The passive fuel cell includes a pair of tanks, current collectors, end plates and a membrane electrode assembly (MEA) in the middle (see Fig. 1). During the cell operation, the e-fuel containing V^{2+} ions is fed to the anode and then oxidized to V^{3+} ions, releasing one electron, according to:

$$V^{2+} \rightarrow V^{3+} + e^{-} E_a^0 = -0.26\text{V} \quad (1)$$

Followed by this, the released electron is then transported to the cathode side, while the proton also migrates across the membrane. At the cathode, the e-fuel containing VO_2^+ ions meets the protons and electrons, where the following reaction then takes place:

$$VO_2^+ + 2H^+ + e^- \rightarrow VO^{2+} + H_2O E_c^0 = 1.00\text{V} \quad (2)$$

The overall reaction inside this cell is:

$$VO_2^+ + 2H^+ + V^{2+} \rightarrow VO^{2+} + V^{3+} + H_2O\,\Delta E = 1.26\text{V} \quad (3)$$

This e-fuel cell, using e-fuels of different compositions on either side, provides a theoretical voltage of 1.26 V, which surpasses many conventional alcohol fuel cells [16].

3 Experiments

3.1 Preparation of MEA

The MEAs were prepared for the single passive fuel cell (2.0 × 2.0 cm^2) and two-cell stack (2.0 × 4.0 cm^2), which was composed of a piece of Nafion 115 sandwiched between two pieces of graphite felts. Before use, the graphite felt (AvCarb G100, Fuel Cell Store, USA) was heated in a muffle furnace for 5 h at 500 °C [10]. The Nafion 115 was pretreated as previously reported to facilitate proton transport [10].

3.2 Cell Assembling and Testing

In this study, the single cell consisting of a pair of acrylic e-fuel tanks, graphite current collectors, and stainless-steel end plates was fabricated, which is similar to the ones reported previously [27]. On the top of the acrylic e-fuel

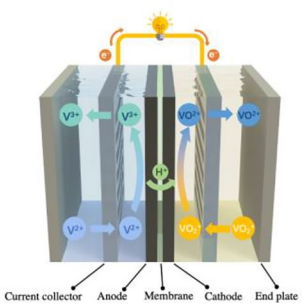

Fig. 1 Working principle of the passive e-fuel cell

tanks (20.0 mL), two holes were drilled for e-fuel injection. Using a similar design, the two-cell stack was consisted of two single cells. However, to reduce the overall size of the stack, the volume of the tank was changed to 4.0 mL and the end plates were eliminated. The e-fuel was prepared by firstly dissolving vanadyl sulfate into H_2SO_4 and then charging using a typical flow cell [10]. All of the electrochemical tests reported in this study were performed by an Arbin BT2000. Before the electrochemical tests, the cell was firstly pre-cooled inside a low-temperature testing chamber until it reached the desired temperature. The cooling process was carefully controlled by adjusting the environment temperature, and all temperatures reported in this study are cell temperatures. After the pre-cooling process, the pre-cooled e-fuels were injected into the cell for further testing.

4 Results and Discussion

4.1 General Performance of the Passive Fuel Cell

In this work, the general performance of this cell at − 20 °C is shown in Fig. 2. Different from the conventional fuel cells that operate in sub-zero environment, the cell presented here excludes any auxiliary equipment, including pumps and heaters. It follows a cold-start free operating strategy so that it starts generating electricity immediately when it is needed without any delay. Such an operation strategy not only provides the cell with a short response time, but also gives the system a higher efficiency due to the exclusion of any additional processes or equipment. Nevertheless, even with this unique operating strategy, an open-circuit voltage (OCV) of 1.49 V and a peak power density (PPD) of 110.34 $mW{\cdot}cm^{-2}$ are achieved, presenting the potential of this cell for application in sub-zero environments.

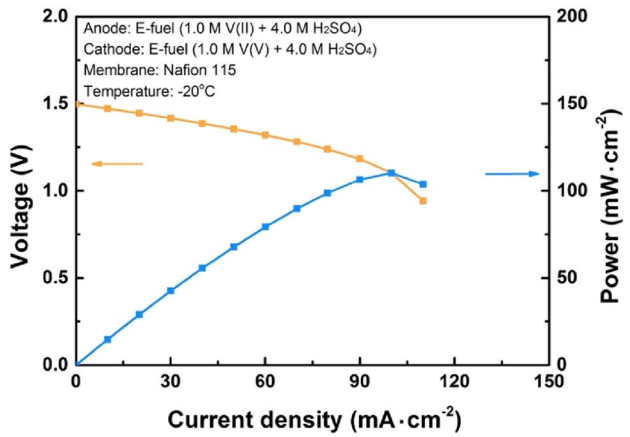

Fig. 2 General performance of the e-fuel cell at − 20 °C

In addition, as can be seen in Table S1 (Supporting Information), the cell also achieves much better performance with a significantly broader operational temperature range than other conventional liquid fuel cells, where the common alcohol fuel cells are unable to generate electricity under the same condition [17–20]. Impressively, when compared to our previously reported e-fuel cell system [11], the present work, by substituting oxygen with another liquid e-fuel on the cathode side, significantly boosts the cell performance even without the assistance of any pumps. Such outstanding performance therefore validates this system as a promising technology for commercialization.

4.2 Effects of E-fuel Composition

The e-fuel composition is important for both the cell performance and its specific energy [21]. Hence, the e-fuels with different concentrations of V(II)/V(V) ions were first fed into the cell for study (Fig. 3(a)), where the e-fuel with the highest concentration (1.0 M V(II)/V(V)) is found to achieve the best cell performance (OCV: 1.49 V, PPD: 211.03 $mW{\cdot}cm^{-2}$). This enhanced cell performance with the increment of V(II)/V(V) ions concentration is attributed to the improved mass transport inside leading to a lower concentration polarization. This is mainly due to the enlarged concentration difference between electrode surface and the tank, thereby intensifying the diffusion process [22]. In addition, the higher concentration of reactive species also contributes to the rise of OCV in accordance with the Nernst equation [23, 24]. Hence, the cell using the e-fuel of higher V(II)/V(V) ions concentration is found to present better performance. Additionally, the effect of H_2SO_4 concentration has also been examined (Fig. 3(b)). As the H_2SO_4 concentration increases from 1.0 M to 4.0 M, the cell performance also improves, due to the improvement in the e-fuel conductivity with the presence of more protons [25]. However, when the H_2SO_4 concentration is further increased to 5.0 M, no obvious performance enhancement is observed. Such a change of trend is ascribed to the fact that higher H_2SO_4 concentration could result in higher e-fuel viscosity, thereby limiting the movement of protons leading to larger mass transport loss [26, 27]. In summary, the e-fuel of 1.0 M V(II)/V(V) in 4.0 M H_2SO_4 is observed to be more suitable and is therefore used for further studies in later sections.

4.3 Effects of Operating Temperature

As discussed, to realize the worldwide application of the e-fuel cell under varied sites and seasons, it is a prerequisite for the system to be able of operating under all-climate conditions, especially in extreme environments [28]. Hence, the cell performance is examined under a varied temperature from 23 to − 20 °C. As shown in Fig. 4(a), with the cell

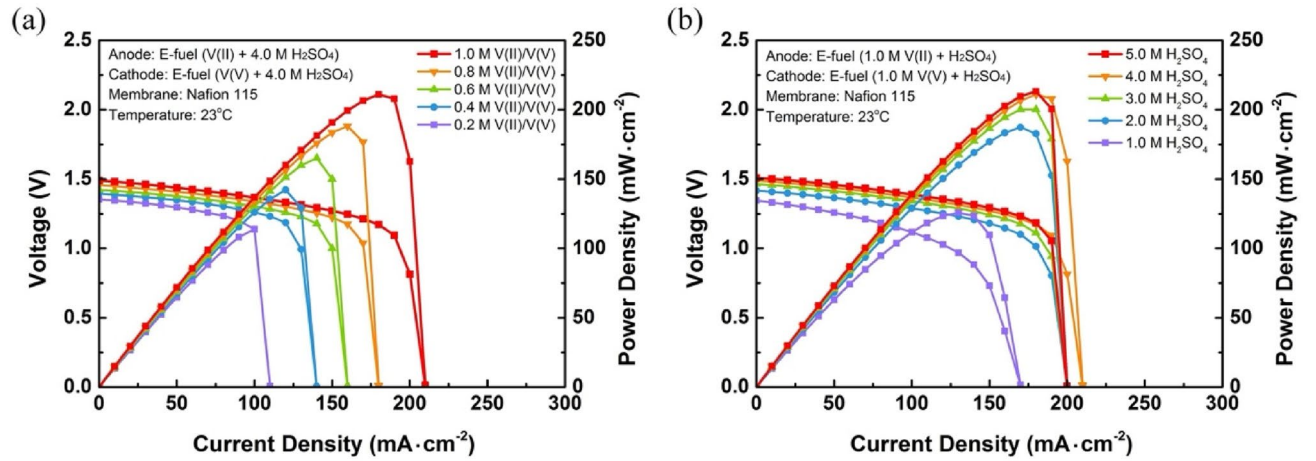

Fig. 3 Effect of **a** V(II)/V(V) ions and **b** sulfuric acid concentrations on cell performance

temperature decreases from 23 to − 20 °C, the PPD also drops from 211.03 to 110.34 mW·cm^{-2}. Such an obvious performance degradation is associated with the increased polarization losses at lower operating temperature. On the one hand, as proved previously, both the e-fuel and membrane conductivities decreases as the operating temperature decreases, which resulted in a higher ohmic resistance [11, 29, 30].

On the other hand, the declined temperature also hampers the diffusion of reactive species, which hinders the mass and charge transport processes inside the cell and thereby leads to a higher mass transport loss and decreased reaction kinetics of the e-fuel oxidation and reduction reactions [31]. To better demonstrate the cell performance under the situation similar to real operating condition, its constant current discharging behaviors are also examined, as presented in Fig. 4(b). The trend of the cell performance varies with the polarization test results, where its discharge capacity declines as operating temperature falls. Overall, the cell is found to be capable of achieving a Faradic efficiency of 22% at 20 °C, which decreases to ~ 3% at − 20 °C. However, it is worth noticing that even at − 20 °C, the cell is able to generate electricity stably without the assistance of any auxiliary equipment. Furthermore, the cell has also been found to have a short response time where it can provide power immediately as needed. These significant merits thereby demonstrate the cell as a viable candidate for power generation under extreme conditions, such as emergency power systems.

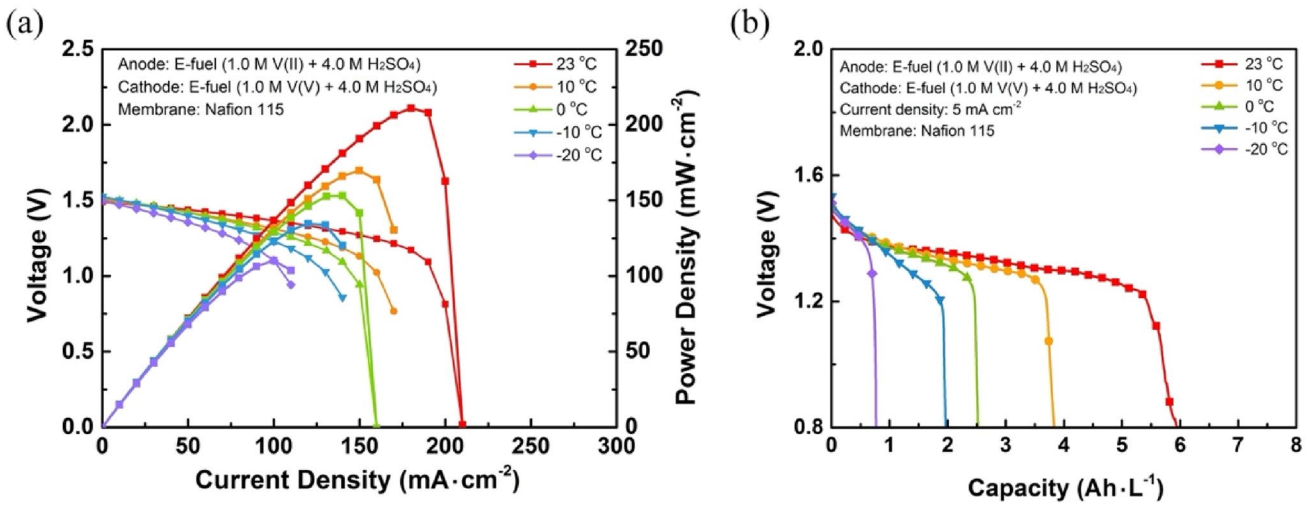

Fig. 4 **a** Polarization curves, and **b** constant-current discharging behavior of the liquid e-fuel cell from 23 to -20 °C

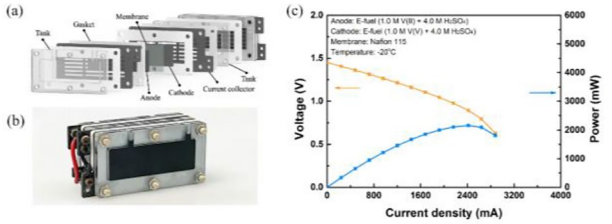

Fig. 5 **a** Design, **b** fabrication, and **c** general performance of the passive e-fuel cell stack

4.4 General Performance of the E-fuel Cell Stack

In previous sections, the e-fuel cell has demonstrated its great potential for application under all-climate conditions. To better illustrate its reproducibility and scalability, a two-cell stack is designed and fabricated (Fig. 5(a)-(b)). First, the performance consistency of the two cells inside the stack is examined (Fig. S1). It is found that the two cells are able to obtain almost identical polarization curves, indicating their good performance consistency and thereby illustrating the superior reproducibility of this system. Furthermore, the cells inside the stack are also found to reproduce ~ 85% of the single cell performance as mentioned above, thereby signifying the outstanding scalability of this system for large-scale application. The slightly reduced stack performance could be attributed to several factors, such as the enlarged membrane size, which can lead to a severe crossover of e-fuel across the membrane. Nevertheless, these results are believed to not only demonstrate but even pave the way for this technology to realize worldwide usage in the future. Thereafter, by connecting these two single cells in parallel, the overall performance of the stack is examined and shown in Fig. 5(c). The stack is found to be capable of attaining an OCV of 1.45 V, a maximum current of 2.88 A, and a peak power of 2.16 W even at − 20 °C. Such superior stack performance has far outperformed most of the conventional passive liquid fuel cell stacks that are even operated at room temperature [32, 33]. The considerable potential of this system therefore has positioned it as a promising candidate for future commercial applications.

4.5 Demonstration for All-Climate Operation

To better exhibit the all-climate operation capability of this system, the stack performance at various operating temperatures is then examined. As shown in Fig. 6(a), from 23 to − 20 °C, while the stack performance decreases with the operating temperature, the system can always maintain stable power generation. Most impressively, the stack achieves a high peak power of 4.44 W at 23 °C. Even at − 20 °C, a peak power of 2.16 W is observed. Though the

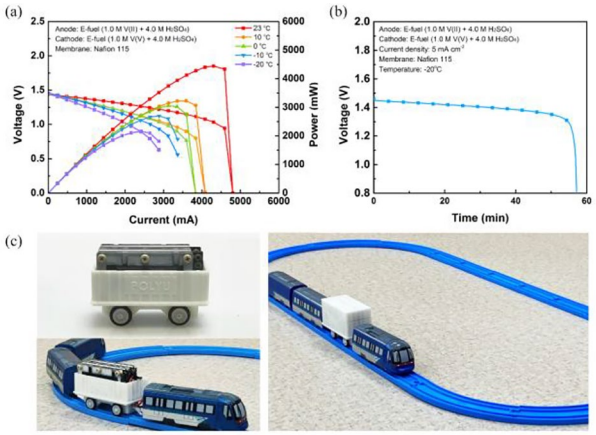

Fig. 6 **a** Polarization curves of the passive e-fuel cell stack at an operating temperature from 23 to -20 °C. **b** Constant-current discharging behavior of the passive e-fuel cell stack at − 20 °C. **c** Demonstration of the passive e-fuel cell stack for powering a toy train

degradation of the stack performance is found as the operating temperature falls, it is worth stressing that this stack is operated under an auxiliary equipment-free operating condition, demonstrating that it is a promising emergency power source. Such a superior stack performance, especially in this sub-zero temperature environment, therefore again justifies the applicability of the designed passive e-fuel cell stack to work under all-climate conditions. Following this, to better simulate the actual operating condition, the constant-current discharging behavior of the stack at − 20 °C is also studied (Fig. 6(b)).

It is found that the cell voltage is able to maintain stably for ~ 60 min before dropping to 0.8 V as a result of the depletion of reactants. Such a relatively short operating duration is due to the low Faradic efficiency as a result of severe e-fuel crossover and side reactions [29]. It also originates from the limited tank size, where the volume of stored e-fuel is constrained. In the future, based on practical needs, the operation duration of the stack can be easily prolonged by simply increasing the tank size. Finally, to further present the practical applicability of the system, the stack is assembled into a 3D printed carriage to power a toy train, as shown in Fig. 6(c). It is demonstrated that the stack is capable of driving the toy train for running stably along the track. Such a demonstration, along with its all-climate operation capability, therefore presents its potential for real-world application under all-climate conditions. However, the scale-up of this system for powering larger devices still faces many challenges. For instance, it is vital for the cell to attain a higher PPD and efficiency to meet the demands of real applications before achieving commercial usage. Meanwhile, its long-term stability in a sub-zero environment also requires further studies.

5 Conclusions

In this study, a passive e-fuel cell is designed and fabricated for power generation under all-climate conditions. Contrary to the conventional cold-start operating strategy, this fuel cell system is free from any auxiliary equipment, while allowing fast start-up with short response time, greatly reducing the system size and cost. Overall, the liquid fuel cell demonstrates stable operation from 23 to − 20 °C. Furthermore, the cell is found to achieve unprecedented performance with a PPD of 110.34 $mW{\cdot}cm^{-2}$ at − 20 °C, surpassing most conventional alcohol fuel cells. Following this, a passive two-cell stack is developed, which not only demonstrates the reproducibility and scalability of this system, but also presents its great commercialization potential. In the future, with further performance improvement, it is expected to become a viable solution for stable power generation, especially in extreme environments.

Supplementary Information The online version contains supplementary material available at https://doi.org/10.1007/s42154-025-00391-7.

Acknowledgements The work described in this paper was supported by a grant from the National Natural Science Foundation of China (No. 52076142), a grant from the NSFC/RGC Joint Research Scheme (N_PolyU559/21), and a grant from Research Institute for Smart Energy at The Hong Kong Polytechnic University (CDB2).

Funding Open access funding provided by The Hong Kong Polytechnic University.

Declarations

Conflict of interest On behalf of all the authors, the corresponding author states that there is no conflict of interest.

References

1. Staffell, I., Scamman, D., Abad, A.V., Balcombe, P., Dodds, P.E., Ekins, P., Shah, N., Ward, K.R.: The role of hydrogen and fuel cells in the global energy system. Energy Environ. Sci. **12**(2), 463–491 (2019)
2. Chikumba, F., Tamer, M., Akyalçın, L., Kaytakoğlu, S.: The development of sulfonated polyether ether ketone (sPEEK) and titanium silicon oxide (TiSiO4) composite membranes for DMFC applications. Int. J. Hydrogen Energy **5**, 96 (2023)
3. Sun, Q., Xu, H., Du, Y.: Recent achievements in noble metal catalysts with unique nanostructures for liquid fuel cells. Chemsuschem **13**(10), 2540–2551 (2020)
4. Goor, M., Menkin, S., Peled, E.: High power direct methanol fuel cell for mobility and portable applications. Int. J. Hydrogen Energy **44**(5), 3138–3143 (2019)
5. Pan, Z., Huang, B., An, L.: Performance of a hybrid direct ethylene glycol fuel cell. Int. J. Energy Res. **43**(7), 2583–2591 (2019)
6. Johánek, V., Ostroverkh, A., Fiala, R.: Vapor-feed low temperature direct methanol fuel cell with Pt and PtRu electrodes: chemistry insight. Renew. Energ. **138**, 409–415 (2019)
7. Park, Y.C., Peck, D.H., Kim, S.K., Lim, S., Lee, D.Y., Ji, H., Jung, D.H.: Operation characteristics of portable direct methanol fuel cell stack at sub-zero temperatures using hydrocarbon membrane and high concentration methanol. Electrochim. Acta **55**(15), 4512–4518 (2010)
8. Song, S., Zhou, W., Li, W., Sun, G., Xin, Q., Kontou, S., Tsiakaras, P.: Direct methanol fuel cells: methanol crossover and its influence on single DMFC performance. Ionics **10**, 458–462 (2004)
9. Nogueira, J.A., Varela, H.: Direct liquid fuel cells—the influence of temperature and dynamic instabilities. Energy Fuels **34**(10), 12995–13009 (2020)
10. Shi, X., Huo, X., Ma, Y., Pan, Z., An, L.: Energizing fuel cells with an electrically rechargeable liquid fuel. Cell Rep. Phys. Sci. **1**(7), 100102 (2020)
11. Shi, X., Huo, X., Esan, O.C., Ma, Y., An, L., Zhao, T.: A liquid e-fuel cell operating at −20° C. J. Power. Sources **506**, 230198 (2021)
12. Tabe, Y., Yamada, K., Ichikawa, R., Aoyama, Y., Suzuki, K., Chikahisa, T.: Ice formation processes in PEM fuel cell catalyst layers during cold startup analyzed by cryo-SEM. J. Electrochem. Soc. **163**(10), F1139 (2016)
13. Cha, H.C., Chen, C.Y., Wang, R.X., Chang, C.L.: Performance test and degradation analysis of direct methanol fuel cell membrane electrode assembly during freeze/thaw cycles. J. Power. Sources **196**(5), 2650–2660 (2011)
14. Borup, R., Meyers, J., Pivovar, B., Kim, Y.S., Mukundan, R., Garland, N., Myers, D., Wilson, M., Garzon, F., Wood, D.: Scientific aspects of polymer electrolyte fuel cell durability and degradation. Chem. Rev. **107**(10), 3904–3951 (2007)
15. Sharaf, O.Z., Orhan, M.F.: An overview of fuel cell technology: Fundamentals and applications. Renew. Sust. Energ. Rev. **32**, 810–853 (2014)
16. Shi, X., Huo, X., Esan, O.C., Dai, Y., An, L., Zhao, T.: Manipulation of electrode composition for effective water management in fuel cells fed with an electrically rechargeable liquid fuel. ACS Appl. Mater. Interfaces **14**(16), 18600–18606 (2022)
17. Fang, Y., Qi, J., Wang, F., Hao, Y., Zhu, J., Zhang, P.: Highly durable passive direct methanol fuel cell with three-dimensional ordered porous NiCo2O4 as cathode catalyst. ChemElectroChem **7**(10), 2314–2324 (2020)
18. Shaari, N., Kamarudin, S.K., Zakaria, Z.: Enhanced alkaline stability and performance of alkali-doped quaternized poly (vinyl alcohol) membranes for passive direct ethanol fuel cell. Int. J. Energy Res. **43**(10), 5252–5265 (2019)
19. Hong, P., Liao, S., Zeng, J., Huang, X.: Design, fabrication and performance evaluation of a miniature air breathing direct formic acid fuel cell based on printed circuit board technology. J. Power. Sources **195**(21), 7332–7337 (2010)
20. Ha, S., Adams, B., Masel, R.: A miniature air breathing direct formic acid fuel cell. J. Power. Sources **128**(2), 119–124 (2004)

21. Wu, Q., Zhao, T., Chen, R., Yang, W.: A microfluidic-structured flow field for passive direct methanol fuel cells operating with highly concentrated fuels. J. Micromech. Microeng. **20**(4), 045014 (2010)
22. Rao, A.S., Rashmi, K., Manjunatha, D., Jayarama, A., Pinto, R.: Enhancement of power output in passive micro-direct methanol fuel cells with optimized methanol concentration and trapezoidal flow channels. J. Micromech. Microeng. **29**(7), 075006 (2019)
23. Knehr, K.W., Kumbur, E.: Open circuit voltage of vanadium redox flow batteries: Discrepancy between models and experiments. Electrochem. Commun. **13**(4), 342–345 (2011)
24. Azam, A., Lee, S., Masdar, M., Zainoodin, A.M., Kamarudin, S.: Parametric study on direct ethanol fuel cell (DEFC) performance and fuel crossover. Int. J. Hydrogen Energy **44**(16), 8566–8574 (2019)
25. Yang, W., He, Y., Li, Y.: Performance modeling of a vanadium redox flow battery during discharging. Electrochim. Acta **155**, 279–287 (2015)
26. Bauer, A., Oloman, C., Gyenge, E.: Three-dimensional anode engineering for the direct methanol fuel cell. J. Power. Sources **193**(2), 754–760 (2009)
27. Lawton, J.S., Tiano, S.M., Donnelly, D.J., Flanagan, S.P., Arruda, T.M.: The effect of sulfuric acid concentration on the physical and electrochemical properties of vanadyl solutions. Batteries **4**(3), 40 (2018)
28. Ivanova, N.A., Spasov, D.D., Grigoriev, S.A., Kamyshinsky, R.A., Peters, G.S., Mensharapov, R.M., Seregina, E.A., Millet, P., Fateev, V.N.: On the influence of methanol addition on the performances of PEM fuel cells operated at subzero temperatures. Int. J. Hydrogen Energy **46**(34), 18116–18127 (2021)
29. Shi, X., Dai, Y., Esan, O.C., Huo, X., An, L., Zhao, T.: A passive fuel cell fed with an electrically rechargeable liquid fuel. ACS Appl. Mater. Interfaces **13**(41), 48795–48800 (2021)
30. Shi, X., Esan, O.C., Huo, X., Ma, Y., Pan, Z., An, L., Zhao, T.: Polymer electrolyte membranes for vanadium redox flow batteries: fundamentals and applications. Progr. Energy Combust. Sci. **85**, 100926 (2021)
31. Joh, H.I., Hwang, S.Y., Cho, J.H., Ha, T.J., Kim, S.K., Moon, S.H., Ha, H.Y.: Development and characteristics of a 400 W-class direct methanol fuel cell stack. Int. J. Hydrogen Energy **33**(23), 7153–7162 (2008)
32. Feng, L., Cai, W., Li, C., Zhang, J., Liu, C., Xing, W.: Fabrication and performance evaluation for a novel small planar passive direct methanol fuel cell stack. Fuel **94**, 401–408 (2012)
33. Wang, L., Yuan, Z., Wen, F., Cheng, Y., Zhang, Y., Wang, G.: A bipolar passive DMFC stack for portable applications. Energy **144**, 587–593 (2018)